Silencing of *DUOX* NADPH Oxidases by Promoter Hypermethylation in Lung Cancer

Sylvia Luxen,[1] Steven A. Belinsky,[2] and Ulla G. Knaus[1]

[1]Department of Immunology, The Scripps Research Institute, La Jolla, California and [2]Lovelace Respiratory Research Institute, Albuquerque, New Mexico

Abstract

The development of lung cancer is associated with aberrant promoter methylation and thus transcriptional silencing of many tumor suppressor genes or genes critical for cellular maintenance. Here we report that the NADPH oxidases *DUOX1* and *DUOX2*, which are one of the main sources for reactive oxygen species production in the airway, are frequently silenced in human lung cancer. Screening of lung cancer cell lines revealed loss of *DUOX1* and *DUOX2* expression, which was restored after treatment with 5-aza 2′-deoxycytidine. Two genes, *DUOXA1* and *DUOXA2*, which are transcriptionally and functionally linked to *DUOX*, also showed coordinated down-regulation in lung cancer cells and lung cancer specimen. Bisulfite sequencing and methylation-specific PCR revealed that CpG-rich promoter regions in both *DUOX* genes are hypermethylated. Epigenetic modification of at least one *DUOX* gene was detected in 50% of primary adenocarcinomas. Immunohistochemical analysis of airway sections derived from cancerous and matched healthy tissues confirmed down-regulation of Duox in the ciliated epithelial cells lining the respiratory tract. Reintroduction of functional Duox1 into lung cancer cell lines increased cell migration and wound repair without affecting cell growth. Our results suggest that an area on chromosome 15 that includes *DUOX1, DUOX2*, and their maturation factors is a frequent target for epigenetic silencing in lung cancer. [Cancer Res 2008;68(4):1037–45]

Introduction

Lung cancer is the leading cause of cancer-related deaths worldwide (1–3). Every year, more people succumb to lung cancer than to breast, prostate, and colorectal cancer together (4). In addition to genomic amplification, homozygous deletion, or mutation of proto-oncogenes and tumor suppressors, epigenetic alterations (i.e., histone modification and DNA methylation) contribute to lung carcinogenesis. Aberrant methylation of CpG islands within the promoter region of tumor suppressors, which leads to epigenetic silencing of these genes, has been recognized as a frequent key event in both early-stage and late-stage lung tumor pathogenesis (2, 5–8). More than 40 genes that are inactivated by promoter hypermethylation have been identified (2, 3). Many of these genes are involved in apoptosis, invasion, DNA repair, cell cycle control, Ras signaling, or cell junction maintenance (9–12).

The family of NADPH oxidases comprises seven members, termed Nox1 to Nox5, Duox1, and Duox2. The homology between all members is based on the well-characterized NADPH oxidase domain that is responsible for the production of reactive oxygen species (ROS; refs. 13, 14). Duox proteins feature an additional extracellular peroxidase domain, with homology to myeloperoxidase and lactoperoxidase (15). Duox2 is mainly expressed in barrier epithelia of the colon, rectum, salivary gland ducts, and thyroid glands (16), whereas Duox1 is predominantly found in the airways and thyroid. Both Duox isoforms, which are 83% homologous in their primary sequence, are located in close proximity on human chromosome 15 (17–19). Recently, a maturation factor for Duox2, termed DuoxA2, was described (20). DuoxA2 is located on the same chromosome in a head-to-head arrangement with Duox2 and is necessary for the posttranslational processing and enzymatic activity of Duox2. A similar role has been proposed for a newly identified maturation factor for Duox1, termed DuoxA1, which is also located in head-to-head arrangement with Duox1 on chromosome 15q15. The activation of Duox proteins leads to calcium-dependent hydrogen peroxide generation into the extracellular milieu. Some of the proposed functions include host defense, promotion of wound healing in the airways, and maintenance of airway homeostasis (16, 21–23). Additionally, Duox may contribute to mucin expression and to acidification of the airway surface liquid (24, 25).

Although knowledge about the cellular functions of Duox1 and Duox2 in the airway epithelium is still limited, these NADPH oxidases seem to have a critical role as regulators of epithelial barrier maintenance. During the development of cancer, many homeostatic processes like water homeostasis and tissue repair are altered (26, 27). Both Duox1 and Duox2 contain CpG-rich promoter regions, making these genes potential targets for aberrant regulation in cancer. The purpose of this study was to assess whether members of the Duox gene family are silenced in lung cancer and the effect that the modulating activity of these genes has on epithelial function in the cancer cell.

Materials and Methods

Cell lines and cell culture. Primary SAEC and NHBE were obtained from Cambrex. Immortalized primary lung epithelial cells SALE and BEAS-2B were gifts from W.C. Hahn (Department of Medicine, Harvard Medical School, Boston, MA) and T. Bigby (Department of Clinical Medicine, University of California San Diego, San Diego, CA; ref. 28). Cells were grown in SABM plus SAGM single quots (Cambrex). NHBE cells were cultivated in BEBM plus BEGM single quots (Cambrex). Lung cancer cell lines NCI-H292, NCI-H727, NCI-H441, NCI-H460, NCI-H661, NCI-H157, A549, Calu-3, NCI-H69, NCI-H82, SHP-77, and UCLA-P3 were from American Type Culture Collection or gifts from F.J. Piedrafita (Sidney Kimmel Cancer Center, La Jolla, CA) and R.A. Reisfeld (Department of Immunology, The Scripps Research Institute, La Jolla, CA). Most cell lines were propagated in RPMI 1640 (Invitrogen) and 10% FCS and 10 mmol/L HEPES (Invitrogen), except

Note: Supplementary data for this article are available at Cancer Research Online (http://cancerres.aacrjournals.org/).

Requests for reprints: Ulla G. Knaus, Department of Immunology, The Scripps Research Institute, 10550 North Torrey Pines Road, La Jolla, CA 92037. Phone 858-784-9281; Fax: 858-784-9580; E-mail: uknaus@scripps.edu.

doi:10.1158/0008-5472.CAN-07-5782

A549 and Calu-3, which were cultured in Ham's F12 or MEM (Invitrogen) containing 10% FCS, 10 mmol/L HEPES, and 1 mmol/L sodium pyruvate.

Tissue samples and immunohistochemistry. Eleven paired specimens of primary lung carcinomas and adjacent noncancerous tissue were obtained from the Cooperative Human Tissue Network (Vanderbilt University Medical Center, Nashville, TN), which is funded by National Cancer Institute. Other investigators may have received specimens from the same subjects. In addition, 39 primary adenocarcinomas from Lovelace Respiratory Research Institute were also studied. All tissue samples were collected from surgical resections, quick-frozen, and stored in liquid nitrogen immediately after excision. Classification was deduced from pathology reports accompanying the coded tissue samples and tumors were staged according to the tumor-node-metastasis staging system by the American Joint Committee on Cancer. Immunohistochemical studies were done on paired tumor and adjacent tissue specimens (Cooperative Human Tissue Network). Deparaffinized sections containing airway crosscuts were stained with anti-Duox and subsequent biotin-streptavidin detection as in ref. 29. The anti-Duox antibody was raised in rabbits to amino acid residues 775 to 1,026 of hDuox1. Visualization was done with 3-amino-9-ethylcarbazole (Sigma). As negative control, immunohistochemistry was done with preimmune serum.

Nucleic acid extraction. Total RNA and genomic DNA from primary cells and cell lines were isolated with RNeasy Kit or DNeasy Tissue Kit (Qiagen). Total RNA from tissue specimens was isolated with a combination of phenol-chloroform and spin-column purification. Three cuts at different positions were done on each tissue. Genomic DNA was isolated simultaneously with total RNA from the same tissue specimen. Integrity of genomic DNA was confirmed by Alu sequence PCR.

Qualitative and quantitative PCR. cDNA was prepared either with SuperScript II (Invitrogen) or High Capacity cDNA reverse transcription kit (Applied Biosystems) and PCR was done using Taq DNA Polymerase (New England Biolabs) or GoTaq Flexi DNA Polymerase (Promega). Primer sequences and cycling parameters are described in Supplementary Table S1. PCR products generated from tissue specimen cDNA were continually measured with an ABI PRISM 7900 Sequence Detection System (Applied Biosystems). Each sample triplicate was probed for Duox1 (Hs00213694_m1, Applied Biosystems), DuoxA1 (Hs00328806_m1), and Duox2 (Hs00204187_m1) and was normalized against human actin (Hs99999903_m1). Relative *DUOX1, DUOX2*, and *DUOXA1* [gene of interest (GOI)] mRNA amounts in the different tissue samples were standardized against the amount of actin mRNA and expressed as $\Delta CT = (CT_{\beta\text{-actin}} - CT_{GOI})$. The mRNA copy ratio of gene of interest to actin was calculated as $2^{\Delta CT}$ and normalized to the highest expression of the respective GOI.

Bisulfite modification and methylation analysis. Genomic DNA was subjected to bisulfite treatment using the EZ DNA Methylation Kit (Zymo Research). CpG islands in the promoter regions of *DUOX1, DUOX2, DUOXA1*, and *DUOXA2* were identified by using CpG island searcher (30). A CpG island was defined by the following criteria: GC >55%, observed CpG/expected CpG >0.65, and length >500 bp. For methylation-specific PCR (MSP), universal primers unbiased for potential CpG conversion sites were used to amplify a larger fragment of the promoter region of *DUOX1* (Universal-a: −262 to +58; Universal-b: −256 to +69) and *DUOX2* (Universal-a: −566 to +65, Universal-b: −327 to −76), respectively. This product was used as template for subsequent MSP and unmethylation-specific PCR (USP) reactions. For bisulfite sequencing, modified genomic DNA was subjected to PCR using the bisulfite sequencing PCR primer set, amplifying a region from −894 to +1411 (*DUOX1*) or −755 to −52 (*DUOX2*; see Supplementary Table S1). The PCR amplicons were gel purified with the Pure Link Quick Gel Extraction Kit (Invitrogen) and subcloned into pCR4-TOPO (Invitrogen). Methprimer software was used to design the biased MSP, USP, and BSP primers (31).

5-Aza-2′-deoxycytidine and trichostatin A treatment. Lung cancer cell lines were incubated in medium containing 5% FCS in the presence or absence of 1 μmol/L 5-aza-2′-deoxycytidine (Aza; Sigma) or 5 ng/mL trichostatin A (Sigma). The medium was changed every 24 h and replenished with fresh Aza or trichostatin A. Cells were harvested after 2 and 5 days of trichostatin A and Aza treatment, respectively, and RNA or protein was isolated for further analysis.

Western blot analysis. Whole-cell lysates were electrophoresed and blotted as described (32). Immunoblots were probed with anti-Duox, anti–c-Myc (Santa Cruz Biotechnology), or anti–α-tubulin (Sigma) antibodies. Secondary antibodies were horseradish peroxidase–conjugated goat anti-rabbit or goat anti-mouse (Southern Biotech).

Determination of H_2O_2 production. Extracellular H_2O_2 in the presence or absence of 2 μmol/L ionomycin (Sigma) or 1 μmol/L thapsigargin (Invitrogen) was measured for 30 min as previously described (32).

Lentivirus production and cell infection. Human Duox1 and DuoxA1 (DQ 489735) were cloned into the CGW lentiviral expression vector (provided by B.E. Torbett, Department of Molecular and Experimental Medicine, The Scripps Research Institute, La Jolla, CA). Virus particles were produced as described elsewhere (33). Duox1- and DuoxA1-deficient lung cancer cell lines A549 and H157 were incubated with viral supernatant in the presence of polybrene (4 μg/mL; refs. 33, 34).

3-(4,5-Dimethylthiazol-2-yl)-2,5-diphenyltetrazolium bromide assay. A549 and H157 cells were seeded in triplicate and grown for up to 5 days in 0.5% Ham's F12 and 2% RPMI, respectively. Proliferation was measured by reduction of 3-(4,5-dimethylthiazol-2-yl)-2,5-diphenyltetrazolium bromide (MTT; Sigma) into formazan. Cells were incubated with 0.5 mg/mL MTT for 30 min before the precipitate was dissolved in DMSO. The absorbance (540 nm) of the solution was determined spectrophotometrically (Synergy HT, Bio-Tek Instruments).

Transwell migration. Migration experiments were done on Transwell semipermeable membranes (8 μm, Corning Costar Transwell Clear), which were coated with 0.15 μg/μL human placenta collagen type IV. Briefly, lung cancer cell lines expressing control vector, DuoxA1, or Duox1/DuoxA1 were suspended in 0.5% fetal bovine serum (FBS)–containing medium. Cells (1×10^5) were plated on top of the insert and directional migration was induced by adding 10% FBS–containing medium to the bottom chamber. Cells were cultured at 37°C for 2 h (H157) or 3.5 h (A549). The remaining cells on top of the insert were removed and cells adherent to the bottom membrane were fixed, stained with Quik-Dip (Mercedes Medical), and quantified.

Wound closure assay. Duox1/DuoxA1–infected lung cancer cell lines or EV control cell lines were grown to confluency on photoetched coverslips (Bellco Glas, Inc.) precoated with bovine fibronectin (20 ng/mL; Sigma). After generation of a linear wound, pictures were taken at the same positions using a phase-contrast microscope at the indicated times. Wound areas were measured in triplicate using Metamorph 6.2 software (Molecular Devices Corporation).

Statistical analysis. Data are shown as mean ± SE. Differences in hydrogen peroxide production per milligram of protein per hour, cell migration rates, and transcript levels were assessed by using a two-tailed Student's *t* test. $P < 0.05$ was regarded as statistically significant. Significance levels were *, $P < 0.05$; **, $P < 0.01$; and ***, $P < 0.001$.

Results

Loss of *DUOX* expression in human lung cancer cell lines. Human primary lung epithelial cells (SAEC and NHBE), immortalized human lung epithelial cells (BEAS-2B and SALE), and several lung cancer cell lines were examined to determine if the expression or activity of Duox enzymes is altered during lung carcinogenesis. *DUOX1* expression was reduced or absent in 9 of 12 lung cancer cell lines, whereas abundant transcript was present in normal and immortalized lung epithelial cells (Fig. 1*A*). Expression of this gene was reduced or lost in three small-cell lung cancer cell lines (H69, H82, and SHP-77) and six of nine non–small-cell lung cancer cell lines. Expression of the closely related NADPH oxidase *DUOX2* and the Duox maturation factors *DUOXA1* and *DUOXA2*, which are located adjacent to *DUOX1* on chromosome 15, was also assessed. *DUOX2* was expressed, albeit at lower levels than *DUOX1*, in normal and immortalized cell lines (Fig. 1*A*). In most lung cancer cell lines, *DUOX2, DUOXA1*, or *DUOXA2* message was absent. Slight differences in *DUOXA1* or *DUOXA2* expression were observed contingent on the PCR conditions (see Fig. 1*A* and *B*). Only coordinated expression of DuoxA1 with Duox1 and of DuoxA2 with Duox2 will

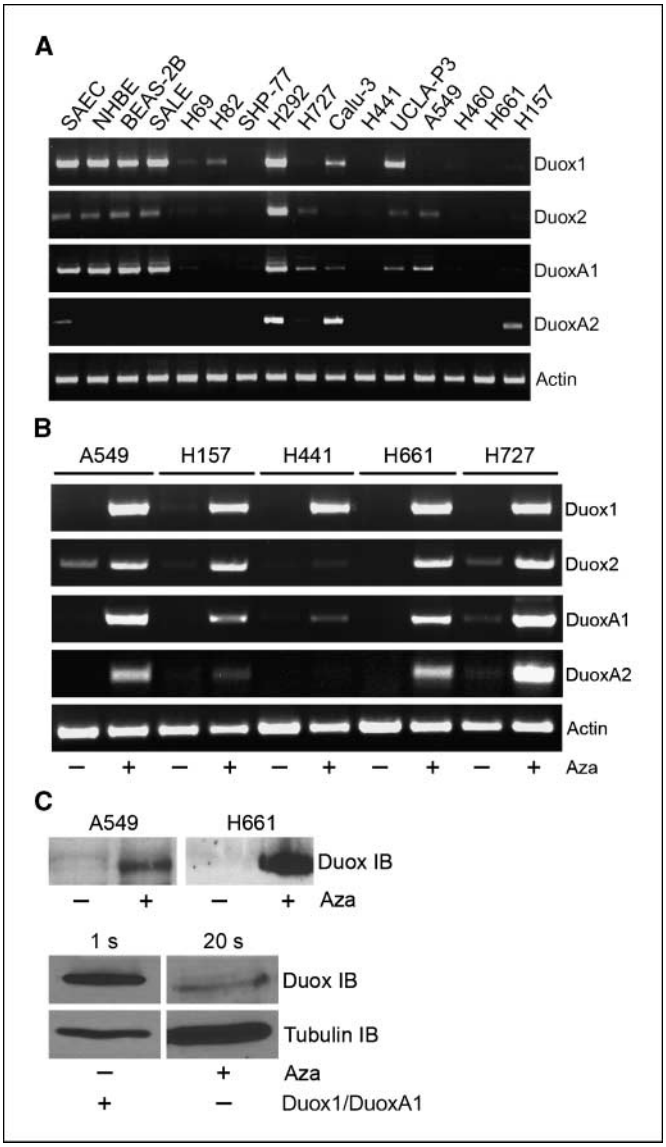

Figure 1. Expression profiles of *DUOX1, DUOX2, DUOXA1*, and *DUOXA2* in lung epithelial cells and recovery of Duox expression in lung cancer cell lines. *A,* reverse transcription-PCR (RT-PCR) was done with primary human lung epithelial cells (SAEC and NHBE), immortalized normal lung epithelial cells (BEAS-2B and SALE), and 12 lung cancer cell lines as indicated. Actin was used as internal control. *B,* recovery of *DUOX1, DUOX2, DUOXA1*, and *DUOXA2* mRNA after treatment with Aza in Duox-deficient lung cancer cell lines. Cells were grown in the presence (+) or absence (−) of 1 μmol/L Aza for 5 d. Gene expression was probed by RT-PCR with actin as control. *C,* immunoblot analysis (*IB*) of Duox expression in lung cancer cell lines A549 and H661 after treatment with 1 μmol/L Aza for 5 d. *Top,* 150 μg of total lysate were loaded on each lane. *Bottom,* H661 cells were grown in the presence of 1 μmol/L Aza for 5 d or transfected with Duox1 and DuoxA1 for 48 h. For each condition, 50 μg of total cell lysate were loaded per lane. Immunoblots were probed with anti-Duox and anti-tubulin antibodies. Proteins were visualized by ECL with exposure times ranging from 1 to 20 s.

allow for maturation of the NADPH oxidase and translocation of a functional enzyme to the plasma membrane. Thus, our results indicate that only the cancer cell line H292 contains a functional oxidase. Reduction in Duox protein levels and functional assays for Duox-mediated ROS generation confirmed this notion.[3]

[3] S. Pacquelet and M. Lehmann, unpublished observations.

Recovery of Duox1 expression in lung cancer cell lines. CpG islands were identified in the promoter regions of *DUOX1, DUOX2*, and their respective maturation factors. Lung cancer cell lines were treated with the methyltransferase inhibitor 5′-aza-2′-deoxycytidine (Aza) for 5 days to determine if expression of these genes was being regulated by promoter hypermethylation. Aza treatment restored *DUOX1* expression in all tested lung cancer cell lines (Fig. 1*B*) and induced *DUOX2, DUOXA1*, and *DUOXA2* expression in four of five cancer cell lines.

Histone acetylation, a dynamic mechanism of epigenetic gene regulation, has been linked to active gene transcription in euchromatin (35). Deacetylation, a process catalyzed by the family of histone deacetylases, mediates transcriptional repression and associates with DNA methylation (36). Treatment of *DUOX*-deficient lung cancer cell lines with the histone deacetylase inhibitor trichostatin A did not increase expression, indicating that histone deacetylation alone is not responsible for the transcriptional silencing of *DUOX* (data not shown).

Cell lysates from Aza-treated cancer cells were probed with anti-Duox antibody (Fig. 1*C, top*). A band of ~180 kDa was observed after Aza treatment. The anti-Duox antibody specifically recognizes Duox, although it will not discriminate between Duox1 and Duox2.[3] Mature Duox enzymes generate H_2O_2 on calcium mobilization, which can be measured using the reduction of homovanillic acid as the readout. Aza-treated A549 or H661 cells, stimulated with ionomycin, produced only minimal amounts of H_2O_2 (data not shown). However, coexpression of Duox1 and DuoxA1 in cancer cell lines yielded substantial H_2O_2 generation on ionomycin stimulation (see Fig. 5*A*). Primary lung epithelial cells up-regulate Duox during ALI-mediated differentiation and thus generate in cell culture conditions much lower amounts of ROS.[3] We hypothesized that Aza-mediated Duox protein recovery in normal cell culture conditions might be too modest to support function. A comparison of protein levels achieved by Aza treatment versus exogenous Duox1 expression confirmed this notion. Immunoblots detected Duox protein after 1 s of enhanced chemiluminescence (ECL) exposure in cell lysates derived from H661 cells transiently transfected with Duox1/DuoxA1, whereas Aza-recovered endogenous Duox was barely detectable after 20 s (Fig. 1*C, bottom*). It is also conceivable that the maturation process of Duox, and thus the processing to a fully functional enzyme, is still disturbed in Aza-treated cancer cells. An antibody recognizing endogenous DuoxA1 is not available, which precluded analysis of DuoxA1 protein expression in Aza-treated cells.

The promoters of *DUOX1* and *DUOX2* are hypermethylated in lung cancer cell lines. The reversal of gene silencing by Aza and the fact that *DUOX1* and *DUOX2* both contain a CpG islands suggest that these genes are being regulated through aberrant promoter hypermethylation. The *DUOX* promoter regions 5′ of the transcriptional start site in five lung cancer cell lines that showed Aza-induced gene reexpression (A549, H157, H441, H661, and H727) and in cells expressing endogenous *DUOX* expression (NHBE, SALE, and H292) were sequenced following bisulfite modification (Fig. 2*A*). Bisulfite sequencing of eight individual clones each disclosed very dense *DUOX1* promoter hypermethylation of the 71 analyzed CpG sites in both A549 and H661 cells. Whereas ~30% to 35% of CpG sites in the *DUOX1* promoter region were methylated in H157 cells, primary NHBE showed almost no methylated CpG sites. The bisulfite sequencing revealed less overall methylation at the 39 investigated CpG sites of the *DUOX2* promoter in the three selected cancer cell lines.

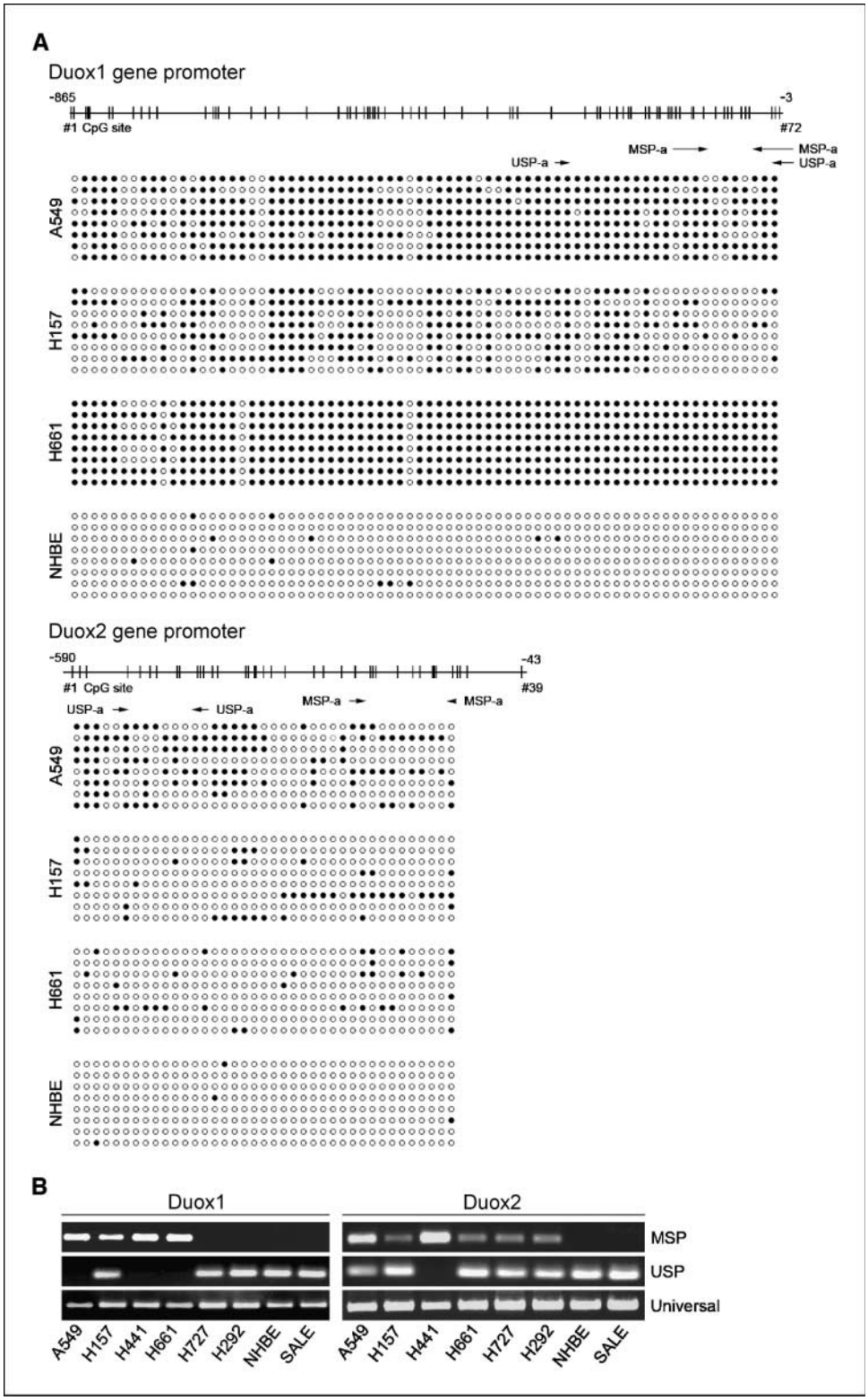

Figure 2. Methylation status of *DUOX1* and *DUOX2* promoters in lung cancer cell lines. Genomic DNA of lung cancer cell lines and normal airway epithelial cells was treated with sodium bisulfite. *A,* results of sodium bisulfite sequencing of three lung cancer cell lines and primary lung epithelial cells. Each row represents one sequenced allele and each circle represents one CpG dinucleotide. The promoter regions upstream of *DUOX1* and *DUOX2* are shown at the top, with vertical bars representing the sites of each analyzed CpG dinucleotide. The PCR products containing 72 and 39 CpG sites, respectively, were cloned and eight individual clones per sample were sequenced. ●, methylated CpG site; ○, unmethylated CpG site. Location of MSP and USP primers (set a) is indicated with arrows. *B,* the methylation status of the promoters of *DUOX1* and *DUOX2* in lung cancer cell lines and in normal lung epithelial cells was analyzed using MSP. Both promoter regions were amplified with primer set Universal-a, followed by PCR using primer set MSP-a and USP-a. Primer locations: Duox1 Universal-a (−262 and +58), Duox1 MSP-a (−96 and +19), Duox1 USP-a (−186 and +21), Duox2 Universal-a (−566 and +65), Duox2 MSP-a (−199 and −18), and Duox2 USP-a (−517 and −402).

Based on the results of the bisulfite sequencing, we carried out methylation specific PCR. Using bisulfite-treated genomic DNA a CpG-rich region of the *DUOX* promoters was amplified with universal primers, which were not biased for CpG sites. The product of this reaction was probed with primers specific for methylated (MSP) or unmethylated sequences (USP). MSP conditions identified the three bisulfite sequenced cancer cell lines and one other *DUOX1*-negative cell line (A549, H157, H661, and H441) as methylation positive within the chosen promoter sequence (Fig. 2*B*). As expected, the amplified promoter region of *DUOX1*-expressing primary lung epithelial cells (NHBE) was not methylated and could be amplified with USP primers. The analyzed

DUOX1 promoter region of cancer cell line H157 was positive for both methylated and unmethylated sequences, which indicates partial methylation, correlating well with the bisulfite sequencing results. Cancer cell line H727, which showed Aza-inducible recovery of *DUOX1* message, was not methylated in this promoter region. This could indicate either that methylation occurred at a different cytosine-rich site of the promoter or that other epigenetic modifications inactivate *DUOX1* gene transcription in these cells. MSP results were confirmed with the second primer set (data not shown). MSP of the *DUOX2* promoter revealed that primary lung epithelial cells are negative for methylation, whereas all tested lung cancer cell lines are at least partially methylated. Bisulfite sequencing results and strong MSP signals for *DUOX2* correlated well in the cancer cell line A549. Cell lines H157 and H661 showed a much weaker MSP signal and less methylation-positive CpG sites, although Aza treatment recovered *DUOX2* similarly. Eight individual clones were bisulfite sequenced and it is possible that not all alleles present in the cancer cell populations were characterized. Unmethylated sequences were detectable in all samples, except one lung cancer cell line (H441), indicating a much higher diversity within the probed *DUOX2* promoter sequence than observed in *DUOX1*.

Down-regulation of *DUOX* expression in primary lung cancer. *DUOX* mRNA levels were analyzed in 11 primary tumors derived from non–small-cell lung cancer patients. The histologic type of the cancer and the corresponding stage are listed in Supplementary Table S2. Tumor tissues and paired adjacent tissues were dissected at three different regions and real-time PCR was done with *DUOX*-specific primers. Nine of eleven patients showed a statistically significant reduction of *DUOX1* expression in tumor tissue compared with the corresponding adjacent tissue (Fig. 3*A*; $P < 0.038$). One patient displayed lower *DUOX1* expression in lung tumor tissue that was not significantly different from adjacent tissue, whereas *DUOX1* mRNA levels of another patient were elevated in cancer tissue when compared with adjacent tissue. *DUOXA1*, which is essential for Duox1 function, showed a similar profile of down-regulation in primary lung cancers (Fig. 3*B*; $P < 0.02$), supporting the premise that expression of Duox1 and DuoxA1 may be linked. Analysis of *DUOX2* also showed statistically significant lower transcript levels in lung cancer tissue in 7 of 11 patients (Fig. 3*C*; $P < 0.034$). Two patients retained *DUOX2* expression while losing *DUOX1* and *DUOXA1* expression. Taken together, these results suggest that expression of *DUOX1, DUOXA1*, and *DUOX2* is significantly reduced in lung tumors.

Decrease of Duox protein in tumorigenic airway tissues. Immunohistochemical staining on paired adjacent and tumor tissue samples derived from two patients was done to evaluate the relationship between *DUOX* expression and protein levels. Duox was detected predominantly in ciliated epithelial cells lining the airways in histologically normal-appearing tissue from patients 11 and 7 (Fig. 4*A*). Considerably weaker staining was observed in the corresponding airways of tumor samples derived from the same patients. No staining of airway cells was detected when using Duox preimmune serum. Limited amounts of tissue precluded analysis of additional specimens.

Methylation of *DUOX* in primary tumors. The relationship between expression and methylation of *DUOX1* in primary tumors was determined by MSP. Five patients, whose tumors showed significant down-regulation of *DUOX1* in quantitative PCR, were chosen for MSP and USP analysis. *DUOX1* hypermethylation was detected in all tumors (Fig. 4*B*). Methylated alleles of *DUOX1* were seen in one of five adjacent tissues, suggesting the presence of extensive field cancerization or occult tumor cells in this sample. USP yielded PCR products in all five patient samples (data not shown), which most likely arises from infiltration of nontransformed cells into the tumor (37, 38).

The prevalence for methylation of the *DUOX1* and *DUOX2* genes was also determined in 39 primary lung adenocarcinomas (Fig. 4*C*). Methylation of *DUOX1* and *DUOX2* was seen in 28% and 38% of tumors, respectively. Fifty percent of tumors showed methylation

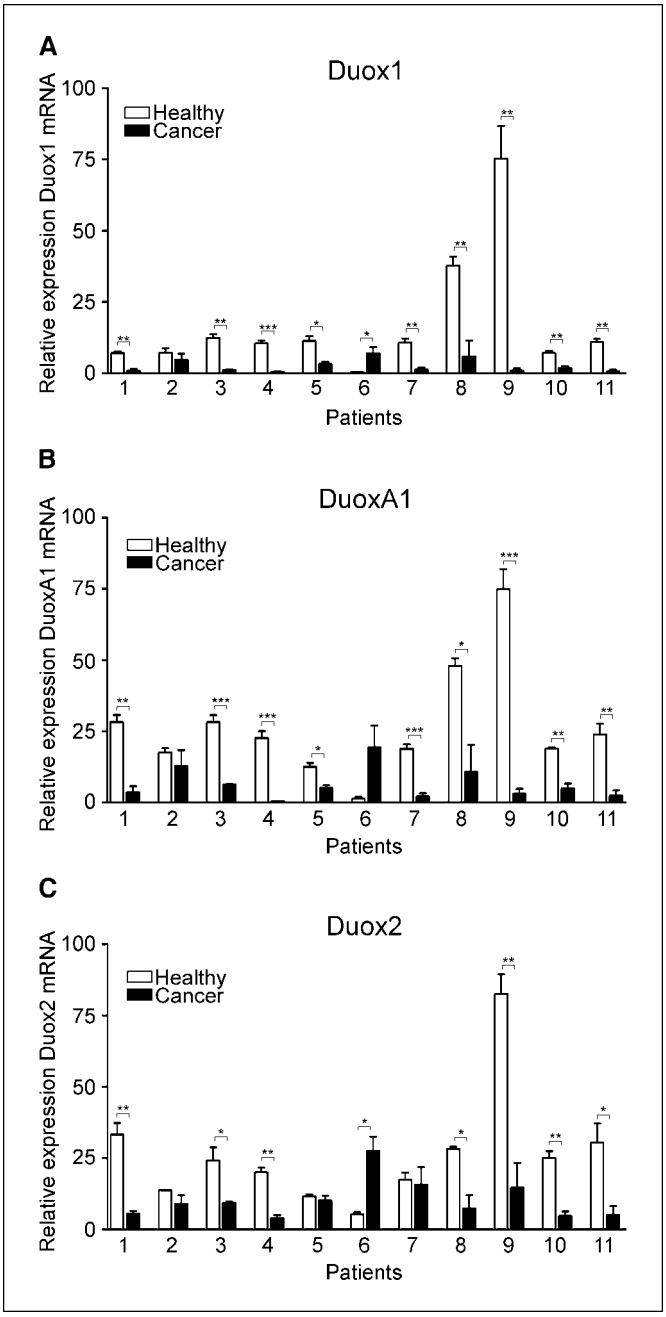

Figure 3. *DUOX1, DUOXA1*, and *DUOX2* expression analysis in paired cancerous and adjacent lung tissue samples. *A* to *C,* quantitative PCR of *DUOX1* (*A*), *DUOXA1* (*B*), and *DUOX2* (*C*) was done on tissue cuts derived from three different regions of the tissue sample in triplicate. Each cut was individually normalized to actin. *Columns,* mean of independent experiments; *bars,* SE ($n = 3$). *, $P < 0.05$; **, $P < 0.01$; ***, $P < 0.001$, two-tailed Student's *t* test.

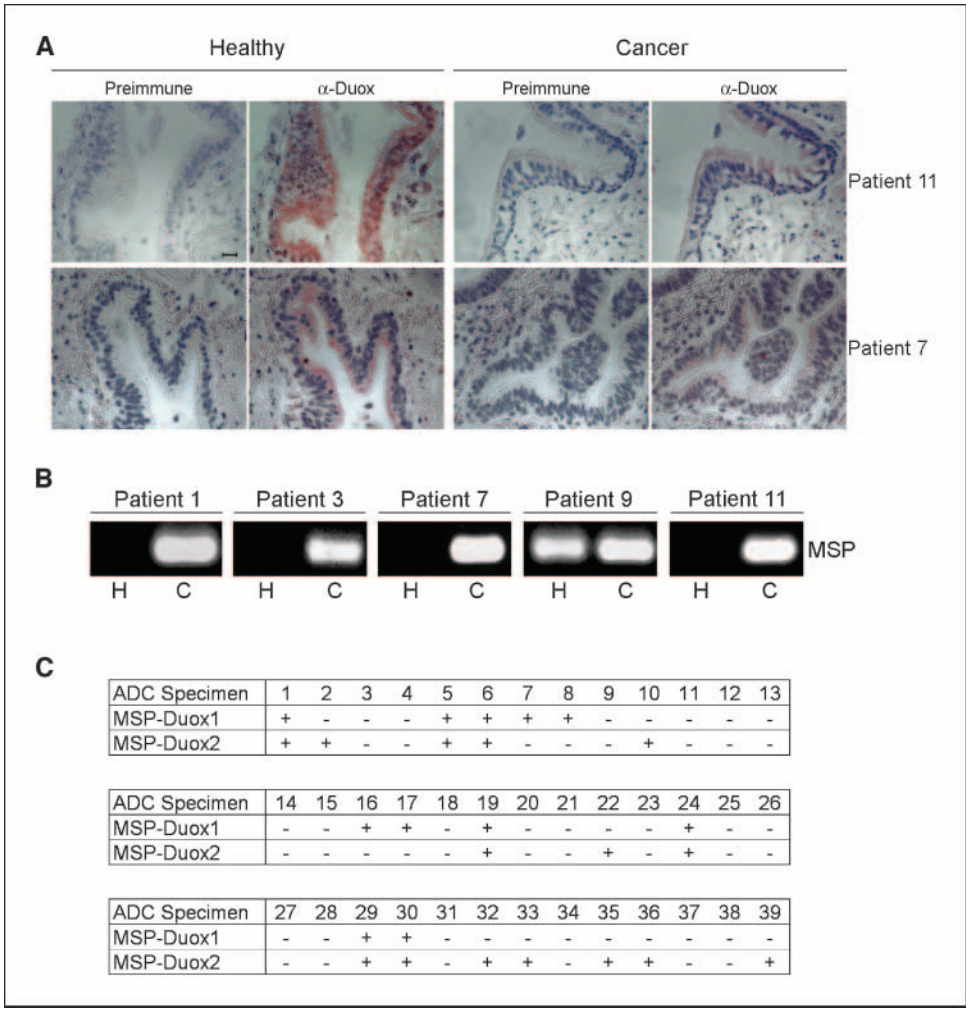

C

ADC Specimen	1	2	3	4	5	6	7	8	9	10	11	12	13
MSP-Duox1	+	-	-	-	+	+	+	+	-	-	-	-	-
MSP-Duox2	+	+	-	-	+	+	-	-	-	+	-	-	-

ADC Specimen	14	15	16	17	18	19	20	21	22	23	24	25	26
MSP-Duox1	-	-	+	+	-	+	-	-	-	-	+	-	-
MSP-Duox2	-	-	-	-	-	+	-	-	+	-	+	-	-

ADC Specimen	27	28	29	30	31	32	33	34	35	36	37	38	39
MSP-Duox1	-	-	+	+	-	-	-	-	-	-	-	-	-
MSP-Duox2	-	-	+	+	-	+	+	-	+	+	-	-	+

Figure 4. Duox expression and promoter analysis in tumor samples. *A,* immunohistochemical staining for Duox in lung tissue cuts derived from two patients (*bar,* 10 μm). Duox protein (*stained red*) is mainly located in ciliated airway cells. *B, DUOX1* promoter methylation analysis in matched healthy (*H*) and cancerous (*C*) tissue samples derived from five patients. Universal and MSP primers were used as described in Fig. 2. *C,* MSP analysis of *DUOX1* and *DUOX2* in 39 primary adenocarcinoma (*ADC*). Methylated sequences were detected with primer sets Duox1 Universal-b (−256 and +69), Duox1 MSP-b (−169 and +5), Duox2 Universal-b (−327 and −76), and Duox2 MSP-b (−240 and −108). +, MSP-PCR product; −, no MSP-PCR product.

in at least one of the *DUOX* genes, and in seven tumors both genes were methylated.

Reconstitution of functional Duox1 results in inducible H_2O_2 production. Attempts have been made to transiently transfect Duox proteins to analyze their regulation in model cell lines. However, the proteins failed to mature and remained nonfunctional or partially functional in the endoplasmic reticulum (39, 40). We cloned DuoxA1, the Duox1 maturation factor, from primary lung epithelial cells. Duox1 and DuoxA1 were inserted into lentiviral expression vectors to allow infection of lung cancer cell lines. Duox1 and DuoxA1 were stably reconstituted in two Duox-deficient lung cancer cell lines (A549 and H157). The transduced cell lines regained the ability to produce H_2O_2 on stimulation with ionomycin or thapsigargin when both oxidase and its maturation factor were present (Fig. 5*A*).

Reintroduction of Duox1 promotes cell migration. Duox1 is the predominant form of Duox in the lung. Therefore, we focused on how loss of Duox1 alters lung epithelial functions. Duox1 has been implicated in airway homeostasis and cell migration (22, 23). Directional migration of vector- or Duox1-expressing cells was analyzed by creating a wound in a confluent monolayer of transduced A549 and H157 cells. Cells expressing Duox1 together with DuoxA1 were able to migrate and close the wound faster than Duox1-deficient cells (Fig. 5*B*). We investigated Duox1-mediated migration more closely by analyzing migration rates in Transwell chambers. Cells were seeded in low-serum medium on top of Transwell membranes and were allowed to migrate to the bottom of the chamber containing serum-rich medium. A549 and H157 cells expressing only DuoxA1 or empty vector migrated into the bottom of the insert, although to a much lower extent than cells expressing functional Duox1/DuoxA1 (Fig. 5*C*). Taken together, these results show that functional Duox1 expression promotes directional migration as well as wound repair.

Proliferation is not influenced by Duox1. The process of wound closure does not only involve cell migration, but necessitates at later stages cell proliferation to repopulate injured areas. Cell proliferation has been linked to increased ROS generation by various cellular sources including the NADPH oxidase Nox1 (41, 42). Because Duox1 has the ability to produce ROS, we assessed whether the introduction of functional Duox1 has an effect on cellular growth rates. The presence of the Duox1/DuoxA1 or DuoxA1 alone did not alter proliferation of A549 and H157 cells when compared with the empty vector–transduced cells (Fig. 5*D*), indicating that restoration of functional Duox1 in selected lung cancer cell lines does not influence cell growth.

Discussion

This study identifies the lung NADPH oxidases *DUOX1* and *DUOX2* as commonly silenced genes in human lung cancer. We

observed loss not only of both *DUOX* genes but also of both *DUOXA* maturation factors in lung cancer cell lines and tumor specimens. The close proximity of *DUOX* and *DUOXA* promoters together with their unique functional relationship may indicate linked gene expression, which is lost on methylation events directed at this chromosomal region. In fact, almost all of the tested lung cancer cell lines did not express functional Duox1 or Duox2. Only H292 cells showed mature Duox expression and

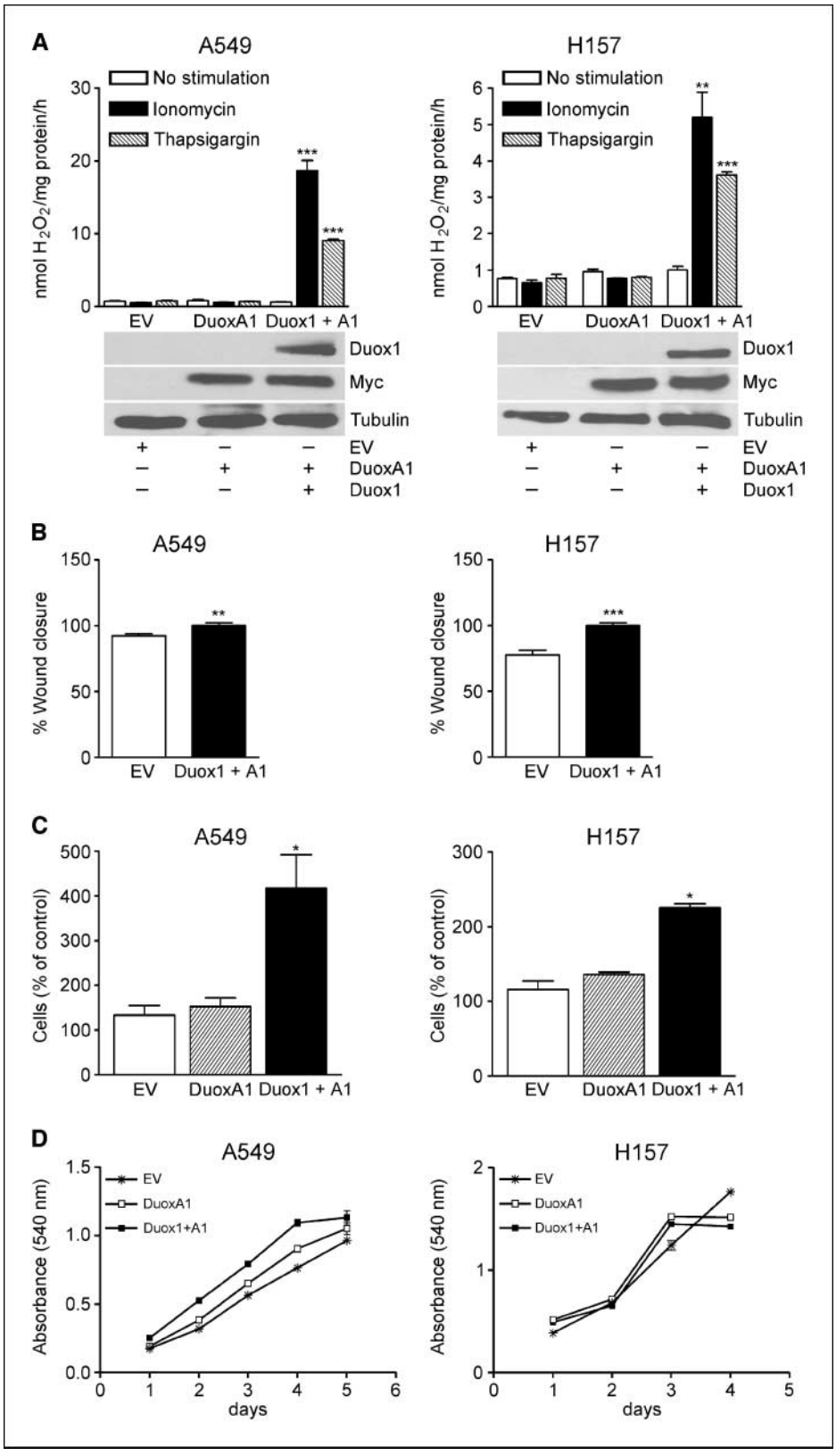

Figure 5. Reintroduction of Duox1 into cancer cell lines promotes wound healing. *A,* Duox1-dependent H_2O_2 production. Lung cancer cell lines A549 and H157 were transduced with empty vector (*EV*), DuoxA1, or Duox1/DuoxA1. H_2O_2 production was determined after stimulation with ionomycin (2 μmol/L) or thapsigargin (1 μmol/L). The immunoblots depict Duox1, DuoxA1 (myc), and tubulin expression in cell lysates. **, $P < 0.01$; ***, $P < 0.001$. *B,* wound closure is accelerated by Duox1. Cell migration across the wound edge after introduction of a linear wound was measured for 9 and 15 h for transduced H157 and A549 cells, respectively. Data were collected from at least nine random fields and are presented as percent closed wound (*bars,* SE). **, $P < 0.01$; ***, $P < 0.001$, compared with the mean of Duox1 + DuoxA1 set as 100% (Student's *t* test). *C,* directional migration is increased by Duox1. Cell migration was initiated by adding FBS to the bottom of the Transwell migration chamber. After 2 and 3.5 h for A549 and H157 cells, respectively, cells on the bottom of the filter were counted. *Columns,* percent of EV control from triplicates of one representative experiment ($n = 3$); *bars,* SE. *, $P < 0.05$. *D,* Duox1 expression does not alter cell proliferation. Transduced A549 and H157 cells were grown in low-serum conditions for up to 5 d. Mitochondrial activity was measured every 24 h spectrophotometrically at 540 nm. Shown is a triplicate of one representative experiment ($n = 3$).

calcium-mediated H_2O_2 generation that was comparable to primary lung epithelial cells.[4] Thus, the normal functions of Duox will be severely disturbed in lung cancer.

The condition of the airway epithelium is of critical importance for the host. It can easily be disturbed through inhaled small particles prevalent in diesel exhaust and cigarette smoke, which are also known to trigger proinflammatory conditions. Continuous exposure to these particles and persistent inflammation can result in an impaired ability to repair damaged tissue, thus resulting in tissue injury and degeneration. Because Duox1 has been associated with airway homeostasis and wound healing (22–24), the transcriptional silencing of *DUOX* might exacerbate the development of abnormal tissue. It is likely that loss of Duox will lead to an impaired ability of airway epithelial cells to react to tissue damage causing increased inflammation. On the other hand, accelerated wound closure by Duox will help in diminishing inflammatory processes. In fact, cigarette smoke has already been connected to decreased migration and impaired wound repair (27).

In addition, ROS provided by Duox may also be required to block cytokinesis in fully differentiated lung epithelium. A recent report linked intracellular ROS accumulation to the establishment of senescence, thereby connecting ROS to tumor suppression (43). This is in contrast to the well-described tumor-promoting activities of ROS, which have been implicated in enhanced cell proliferation and metastasis. Duox reconstitution in lung cancer cell lines did not alter growth rates of two selected lung cancer cell lines; however, Duox might be involved in maintaining the differentiated phenotype and the ability for rapid tissue repair in the airways.

In summary, we here report frequent down-regulation of both Duox NADPH oxidases in lung cancer. Analysis of tumor specimens indicates that aberrant hypermethylation of the *DUOX1* and *DUOX2* promoters is the predominant factor for loss of Duox. Interestingly, all promoters of human *DUOX* or *DUOXA* genes harbor CpG islands. This might make these promoter regions especially susceptible to epigenetic deregulation, particularly in the context of recent findings of Brena et al. (44), who reported that loci at 15q15.1 and 15q22.2, which are in close proximity to the Duox gene cluster at 15q15-21, are aberrantly methylated. Thus, the Duox locus and the surrounding area on chromosome 15 might constitute a potential hotspot for nonrandom CpG island methylation. DNA methylation at these loci may not only mediate gene silencing but may also constitute a preferred target area for chemical carcinogens resulting in DNA damage (45).

[4] S. Pacquelet and M. Lehmann, unpublished observations.

Acknowledgments

Received 10/8/2007; revised 11/26/2007; accepted 12/5/2007.

Grant support: NIH grant AI024838 (U.G. Knaus), CID/CDCP grant CI000095 (U.G. Knaus), and NIH grant RO1 ES008801 (S.A. Belinsky).

The costs of publication of this article were defrayed in part by the payment of page charges. This article must therefore be hereby marked *advertisement* in accordance with 18 U.S.C. Section 1734 solely to indicate this fact.

We thank Drs. M. Trifilo, J. Mols, G. Bokoch, S-T. Lim, and D. Schlaepfer for advice, technical assistance, and access to videomicroscopy equipment; Kieu Do for technical assistance with MSP assays; and Dr. A. Baumann for helpful discussions and K. Schreiber for administrative support.

References

1. Parkin DM, Bray F, Ferlay J, Pisani P. Global cancer statistics, 2002. CA Cancer J Clin 2005;55:74–108.
2. Tsou JA, Hagen JA, Carpenter CL, Laird-Offringa IA. DNA methylation analysis: a powerful new tool for lung cancer diagnosis. Oncogene 2002;21:5450–61.
3. Zochbauer-Muller S, Minna JD, Gazdar AF. Aberrant DNA methylation in lung cancer: biological and clinical implications. Oncologist 2002;7:451–7.
4. Cassidy A, Duffy SW, Myles JP, Liloglou T, Field JK. Lung cancer risk prediction: a tool for early detection. Int J Cancer 2007;120:1–6.
5. Widschwendter M, Jiang G, Woods C, et al. DNA hypomethylation and ovarian cancer biology. Cancer Res 2004;64:4472–80.
6. Machida EO, Brock MV, Hooker CM, et al. Hypermethylation of ASC/TMS1 is a sputum marker for late-stage lung cancer. Cancer Res 2006;66:6210–8.
7. Bowman RV, Yang IA, Semmler AB, Fong KM. Epigenetics of lung cancer. Respirology 2006;11:355–65.
8. Palmisano WA, Divine KK, Saccomanno G, et al. Predicting lung cancer by detecting aberrant promoter methylation in sputum. Cancer Res 2000;60:5954–8.
9. Krunkosky TM, Martin LD, Fischer BM, Voynow JA, Adler KB. Effects of TNFα on expression of ICAM-1 in human airway epithelial cells *in vitro*: oxidant-mediated pathways and transcription factors. Free Radic Biol Med 2003;35:1158–67.
10. Tang X, Wu W, Sun SY, Wistuba II, Hong WK, Mao L. Hypermethylation of the death-associated protein kinase promoter attenuates the sensitivity to TRAIL-induced apoptosis in human non-small cell lung cancer cells. Mol Cancer Res 2004;2:685–91.
11. Belinsky SA. Gene-promoter hypermethylation as a biomarker in lung cancer. Nat Rev Cancer 2004;4:707–17.
12. Zhou XM, Shao SJ, Xu GD, et al. Highly sensitive determination of the methylated p16 gene in cancer patients by microchip electrophoresis. J Chromatogr B Analyt Technol Biomed Life Sci 2005;816:145–51.
13. Lambeth JD. NOX enzymes and the biology of reactive oxygen. Nat Rev Immunol 2004;4:181–9.
14. Donko A, Peterfi Z, Sum A, Leto T, Geiszt M. Dual oxidases. Philos Trans R Soc Lond B Biol Sci 2005;360:2301–8.
15. Harper RW, Xu C, Eiserich JP, et al. Differential regulation of dual NADPH oxidases/peroxidases, Duox1 and Duox2, by Th1 and Th2 cytokines in respiratory tract epithelium. FEBS Lett 2005;579:4911–7.
16. Geiszt M, Witta J, Baffi J, Lekstrom K, Leto TL. Dual oxidases represent novel hydrogen peroxide sources supporting mucosal surface host defense. FASEB J 2003;17:1502–4.
17. Caillou B, Dupuy C, Lacroix L, et al. Expression of reduced nicotinamide adenine dinucleotide phosphate oxidase (ThoX, LNOX, Duox) genes and proteins in human thyroid tissues. J Clin Endocrinol Metab 2001;86:3351–8.
18. De Deken X, Wang D, Many MC, et al. Cloning of two human thyroid cDNAs encoding new members of the NADPH oxidase family. J Biol Chem 2000;275:23227–33.
19. Pachucki J, Wang D, Christophe D, Miot F. Structural and functional characterization of the two human ThOX/Duox genes and their 5′-flanking regions. Mol Cell Endocrinol 2004;214:53–62.
20. Grasberger H, Refetoff S. Identification of the maturation factor for dual oxidase. Evolution of an eukaryotic operon equivalent. J Biol Chem 2006;281:18269–72.
21. Ha EM, Oh CT, Bae YS, Lee WJ. A direct role for dual oxidase in Drosophila gut immunity. Science 2005;310:847–50.
22. Wesley UV, Bove PF, Hristova M, McCarthy S, van der Vliet A. Airway epithelial cell migration and wound repair by ATP-mediated activation of dual oxidase 1. J Biol Chem 2007;282:3213–20.
23. Koff JL, Shao MX, Kim S, Ueki IF, Nadel JA. Pseudomonas lipopolysaccharide accelerates wound repair via activation of a novel epithelial cell signaling cascade. J Immunol 2006;177:8693–700.
24. Schwarzer C, Machen TE, Illek B, Fischer H. NADPH oxidase-dependent acid production in airway epithelial cells. J Biol Chem 2004;279:36454–61.
25. Shao MX, Nadel JA. Dual oxidase 1-dependent MUC5AC mucin expression in cultured human airway epithelial cells. Proc Natl Acad Sci U S A 2005;102:767–72.
26. Comis RL, Miller M, Ginsberg SJ. Abnormalities in water homeostasis in small cell anaplastic lung cancer. Cancer 1980;45:2414–21.
27. Wang H, Liu X, Umino T, et al. Cigarette smoke inhibits human bronchial epithelial cell repair processes. Am J Respir Cell Mol Biol 2001;25:772–9.
28. Lundberg AS, Randell SH, Stewart SA, et al. Immortalization and transformation of primary human airway epithelial cells by gene transfer. Oncogene 2002;21:4577–86.
29. Yuan A, Yu CJ, Luh KT, Kuo SH, Lee YC, Yang PC. Aberrant p53 expression correlates with expression of vascular endothelial growth factor mRNA and interleukin-8 mRNA and neoangiogenesis in non-small-cell lung cancer. J Clin Oncol 2002;20:900–10.
30. Takai D, Jones PA. The CpG island searcher: a new WWW resource. In Silico Biol 2003;3:235–40.
31. Li LC, Dahiya R. MethPrimer: designing primers for methylation PCRs. Bioinformatics 2002;18:1427–31.
32. Martyn KD, Frederick LM, von Loehneysen K, Dinauer MC, Knaus UG. Functional analysis of Nox4 reveals unique characteristics compared to other NADPH oxidases. Cell Signal 2006;18:69–82.
33. Swan CH, Buhler B, Steinberger P, Tschan MP, Barbas CF III, Torbett BE. T-cell protection and enrichment through lentiviral CCR5 intrabody gene delivery. Gene Ther 2006;13:1480–92.
34. Rizzi M, Tschan MP, Britschgi C, et al. The death-associated protein kinase 2 (DAPK2) is up-regulated

during normal myeloid differentiation and enhances neutrophil maturation in myeloid leukemic cells. J Leukoc Biol 2007;81:1599–608.
35. Clayton AL, Hazzalin CA, Mahadevan LC. Enhanced histone acetylation and transcription: a dynamic perspective. Mol Cell 2006;23:289–96.
36. Razin A. CpG methylation, chromatin structure and gene silencing—a three-way connection. EMBO J 1998; 17:4905–8.
37. Chang HC, Cho CY, Hung WC. Down-regulation of RECK by promoter methylation correlates with lymph node metastasis in non-small cell lung cancer. Cancer Sci 2007;98:169–73.
38. Krassenstein R, Sauter E, Dulaimi E, et al. Detection of breast cancer in nipple aspirate fluid by CpG island hypermethylation. Clin Cancer Res 2004;10:28–32.
39. De Deken X, Wang D, Dumont JE, Miot F. Characterization of ThOX proteins as components of the thyroid H(2)O(2)-generating system. Exp Cell Res 2002;273:187–96.
40. Wang D, De Deken X, Milenkovic M, et al. Identification of a novel partner of duox: EFP1, a thioredoxin-related protein. J Biol Chem 2005;280:3096–103.
41. Arbiser JL, Petros J, Klafter R, et al. Reactive oxygen generated by Nox1 triggers the angiogenic switch. Proc Natl Acad Sci U S A 2002;99:715–20.
42. Ranjan P, Anathy V, Burch PM, Weirather K, Lambeth JD, Heintz NH. Redox-dependent expression of cyclin D1 and cell proliferation by Nox1 in mouse lung epithelial cells. Antioxid Redox Signal 2006;8:1447–59.
43. Ramsey MR, Sharpless NE. ROS as a tumour suppressor? Nat Cell Biol 2006;8:1213–5.
44. Brena RM, Morrison C, Liyanarachchi S, et al. Aberrant DNA methylation of OLIG1, a novel prognostic factor in non-small cell lung cancer. PLoS Med 2007;4:e108.
45. Denissenko MF, Chen JX, Tang MS, Pfeifer GP. Cytosine methylation determines hot spots of DNA damage in the human P53 gene. Proc Natl Acad Sci U S A 1997;94:3893–8.